Magnetic Field Influence on Blood Flow in Pathological Vessels: A Computational Study

30th Summer School – Conference “Dynamical Systems and Complexity”

Konstantina Kyriakoudi

Supervisor: M. Xenos

September 5, 2024

University of Ioannina
Department of Mathematics

Outline

Aim of this presentation is the study of hemodynamics in a pathological vessel under the influence of a uniform magnetic field. To solve the system of equations describing the problem, the numerical method of Finite Volumes has been utilized.

Introduction

Introduction

Introduction to Fluid Dynamics

Computational Fluid Dynamics and Fluid Structure Interaction

Computational fluid dynamics (CFD) is a branch of fluid mechanics that uses numerical analysis and data structures to analyze and solve problems that involve fluid flows.

Fluid Structure Interaction (FSI) is the way to describe the interaction between the fluid and the solid interface eg. blood and the arterial wall.

Some of the well-known examples are:

- aerofoil design,
- wind turbines,
- flow in arteries!
- design of mechanical heart valves!

Introduction

Anatomy of an Aneurysm

Anatomy of an Aneurysm

An **aneurysm** is a bulge in a blood vessel caused by a weakness in the blood vessel wall.

- The arterial wall can be weakened by the pressure of the blood.
- The most common locations are the arteries supplying the brain and the heart.
- There's a risk that a larger aneurysm could burst (rupture) and lead to massive internal bleeding.

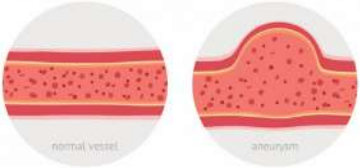

Figure 1: Comparison between a normal and an aneurysmal vessel.

Anatomy of an Aneurysm

Suspicion of an unrupted aneurysm, can be confirmed through diagnostic imaging, such as an Magnetic Resonance Imaging (MRI) [3]. Thus, patients with aneurysm are more likely to be exposed to the effect of the magnetic field.

- Clinical MRI scanners $0.5 - 3.0\ T$.
- Research MRI scanners $7.0 - 11.7\ T$.

This study focuses on fusiform aneurysms.

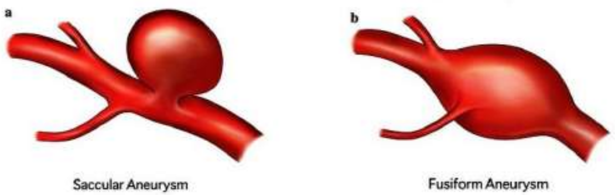

Figure 2: Types of aneurysms.

Mathematical Modelling

Navier-Stokes Equations

The problem can be described by the following system of equations.

continuity equation

$$\frac{\partial \rho}{\partial \tilde{t}} + \frac{\partial(\rho \tilde{u})}{\partial \tilde{x}} + \frac{\partial(\rho \tilde{v})}{\partial \tilde{y}} = 0, \tag{1}$$

x-momentum equation

$$\frac{\partial (\rho \tilde{u})}{\partial \tilde{t}} + \frac{\partial (\rho \tilde{u}\tilde{u})}{\partial \tilde{x}} + \frac{\partial (\rho \tilde{u}\tilde{v})}{\partial \tilde{y}} = -\frac{\partial \tilde{p}}{\partial \tilde{x}} + \left[\frac{\partial}{\partial \tilde{x}}\left(\mu \frac{\partial \tilde{u}}{\partial \tilde{x}}\right) + \frac{\partial}{\partial \tilde{y}}\left(\mu \frac{\partial \tilde{u}}{\partial \tilde{y}}\right)\right] - \sigma \tilde{u} B^2, \tag{2}$$

y-momentum equation

$$\frac{\partial (\rho \tilde{v})}{\partial \tilde{t}} + \frac{\partial (\rho \tilde{u}\tilde{v})}{\partial \tilde{x}} + \frac{\partial (\rho \tilde{v}\tilde{v})}{\partial \tilde{y}} = -\frac{\partial \tilde{p}}{\partial \tilde{y}} + \left[\frac{\partial}{\partial \tilde{x}}\left(\mu \frac{\partial \tilde{v}}{\partial \tilde{x}}\right) + \frac{\partial}{\partial \tilde{y}}\left(\mu \frac{\partial \tilde{v}}{\partial \tilde{y}}\right)\right], \tag{3}$$

- $\tilde{\mathrm{q}} = (\tilde{u}, \tilde{v})$ is the velocity vector,
- p is the kinematic pressure,
- ρ is the density,
- μ is the dynamic viscosity,
- σ is the electrical conductivity,
- B is the magnetic field,
- $\sigma \tilde{u} B^2$ is the x-component of the Lorentz force.

Mathematical Modelling

Dimensionless Equations

Dimensionless Equations

Using the following dimensionless parameters,

$$x = \frac{\tilde{x}}{R}, \quad y = \frac{\tilde{y}}{R}, \quad t = \frac{\tilde{t}}{R/u_0}, \quad u = \frac{\tilde{u}}{u_0}, \quad v = \frac{\tilde{v}}{u_0}, \quad p = \frac{\tilde{p}}{\rho u_0^2}, \quad c = \frac{\rho}{\rho_0}, \qquad (4)$$

u_0 is the characteristic inlet velocity,
R is the inlet length of the aneurysmal geometry.

Dimensionless Equations

The initial system of equations is transformed to a dimensionless form

continuity equation

$$\frac{\partial c}{\partial t} + \frac{\partial (cu)}{\partial x} + \frac{\partial (cv)}{\partial y} = 0, \tag{5}$$

x-momentum equation

$$\frac{\partial u}{\partial t} + \frac{\partial (uu)}{\partial x} + \frac{\partial (uv)}{\partial y} = -\frac{\partial p}{\partial x} + \frac{\partial}{\partial x}\left(\frac{1}{Re}\frac{\partial u}{\partial x}\right) + \frac{\partial}{\partial y}\left(\frac{1}{Re}\frac{\partial u}{\partial y}\right) - Mu, \tag{6}$$

y-momentum equation

$$\frac{\partial v}{\partial t} + \frac{\partial (uv)}{\partial x} + \frac{\partial (vv)}{\partial y} = -\frac{\partial p}{\partial y} + \frac{\partial}{\partial x}\left(\frac{1}{Re}\frac{\partial v}{\partial x}\right) + \frac{\partial}{\partial y}\left(\frac{1}{Re}\frac{\partial v}{\partial y}\right), \tag{7}$$

Re is the *Reynolds* number, $Re = \dfrac{u_0 R}{\nu}$,

M is the magnetic parameter, $M = \frac{\sigma R B^2}{\rho u_0}$

Mathematical Modelling

Generalized Curvilinear Coordinates (GCC)

Applying the generalized curvilinear coordinates (GCCs) transformation, the system of equations under consideration is written in a body–fitted approach. This is possible due to the fact that a local transformation from one domain, e.g. the physical domain, to a normalized one, e.g. the transformed domain, can be obtained, as depicted in **Figure 3**.

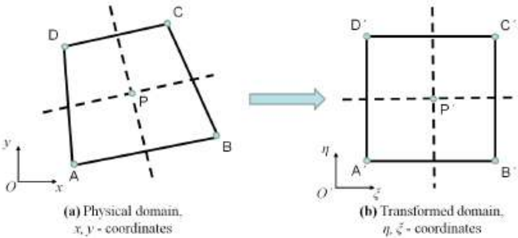

Figure 3: The local transformation from the physical to the transformed domain.

Generalized Curvilinear Coordinates

The problem can be described using the following system of equations.

continuity equation

$$\frac{\partial J}{\partial t} + \frac{\partial U}{\partial \xi} + \frac{\partial V}{\partial \eta} = 0, \tag{8}$$

x-momentum equation

$$\begin{aligned} \frac{\partial (Ju)}{\partial t} + \frac{\partial (Uu)}{\partial \xi} + \frac{\partial (Vu)}{\partial \eta} = -\left(y_\eta \frac{\partial p}{\partial \xi} - y_\xi \frac{\partial p}{\partial \eta} \right) + \frac{\partial}{\partial \xi}\left[\frac{1}{JRe} \left(q_1 \frac{\partial u}{\partial \xi} - q_2 \frac{\partial u}{\partial \eta} \right) \right] \\ + \frac{\partial}{\partial \eta}\left[\frac{1}{JRe} \left(q_3 \frac{\partial u}{\partial \eta} - q_2 \frac{\partial u}{\partial \xi} \right) \right] - MuJ, \end{aligned} \tag{9}$$

y-momentum equation

$$\begin{aligned} \frac{\partial (Jv)}{\partial t} + \frac{\partial (Uv)}{\partial \xi} + \frac{\partial (Vv)}{\partial \eta} = -\left(x_\xi \frac{\partial p}{\partial \eta} - x_\eta \frac{\partial p}{\partial \xi} \right) + \frac{\partial}{\partial \xi}\left[\frac{1}{JRe} \left(q_1 \frac{\partial v}{\partial \xi} - q_2 \frac{\partial v}{\partial \eta} \right) \right] \\ + \frac{\partial}{\partial \eta}\left[\frac{1}{JRe} \left(q_3 \frac{\partial v}{\partial \eta} - q_2 \frac{\partial v}{\partial \xi} \right) \right], \end{aligned} \tag{10}$$

where $U = (u - \dot{x})\, y_\eta - (v - \dot{y})\, x_\eta$, $V = (v - \dot{y})\, x_\xi - (u - \dot{x})\, y_\xi$ and $J = x_\xi y_\eta - x_\eta y_\xi$.

Mathematical Modelling

Boundary Conditions

Boundary Conditions

The boundary conditions for this problem are

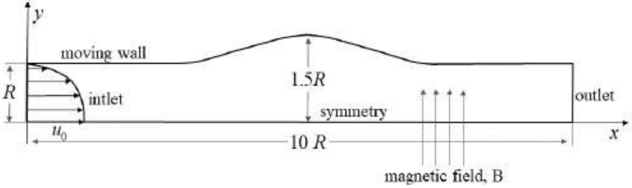

Figure 4: An outline of the geometry and the boundary conditions applied on the aneurysmal model.

- at the inlet: $u(y,t) = \left[1 - \left(\frac{y}{R}\right)^2\right] \times \text{velocity waveform}(t),\ \upsilon = 0,\ \ 0 \leqslant y \leqslant R,$
- at the moving wall : $u = \dot{x},\ \upsilon = \dot{y},\ \ \text{kinematic boundary condition},$
- at the symmetry : $\dfrac{\partial u}{\partial y} = 0,\ \ \upsilon = 0, \text{ for }\ t \geq 0,$
- at the outlet : $p = \text{pressure waveform}(t),\ \dfrac{\partial u}{\partial x} = 0,\ \dfrac{\partial \upsilon}{\partial x} = 0$

Finite Volume Method

The corresponding version of the x-momentum equation is:

$$\frac{Ju - J_0 u_0}{\Delta t} + \left(Uu - \frac{1}{J\,\mathrm{Re}}\left(q_1 \frac{\partial u}{\partial \xi} - q_2 \frac{\partial u}{\partial \eta}\right) + \frac{\partial y}{\partial \eta} p - MuJ\right)_e - \left(Uu - \frac{1}{J\,\mathrm{Re}}\left(q_1 \frac{\partial u}{\partial \xi} - q_2 \frac{\partial u}{\partial \eta}\right) + \frac{\partial y}{\partial \eta} p - MuJ\right)_w$$
$$+ \left(Vu - \frac{1}{J\,\mathrm{Re}}\left(-q_2 \frac{\partial u}{\partial \xi} + q_3 \frac{\partial u}{\partial \eta}\right) - \frac{\partial y}{\partial \xi} p\right)_n - \left(Vu - \frac{1}{J\,\mathrm{Re}}\left(-q_2 \frac{\partial u}{\partial \xi} + q_3 \frac{\partial u}{\partial \eta}\right) - \frac{\partial y}{\partial \xi} p\right)_s = 0, \tag{11}$$

Numerical Considerations:

- a Finite Volume Method algorithm was utilized for the solution
- a numerical code was developed in MATLAB (MathWorks, Natick, MA, USA)
- used parallel programming
- Intel Xeon processors (4210R, 2.40GHz, 24 CPUs)

Results

The following scenarios were studied:

- 4 cardiac cycles
- 2 pulsatilities (low and medium, with a 5.5% and 14% change of the initial diameter)
- gradual increase of the magnetic field at 8 ($B = 0, 4, 8T$)

Additionally, each cardiac cycle is divided in three intervals:

α′ systolic acceleration

β′ systolic deceleration

γ′ diastole

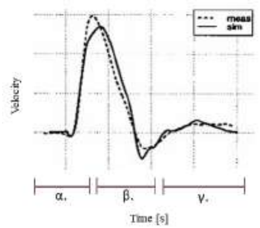

Figure 5: Phases of the cardiac cycle.

Flow Video

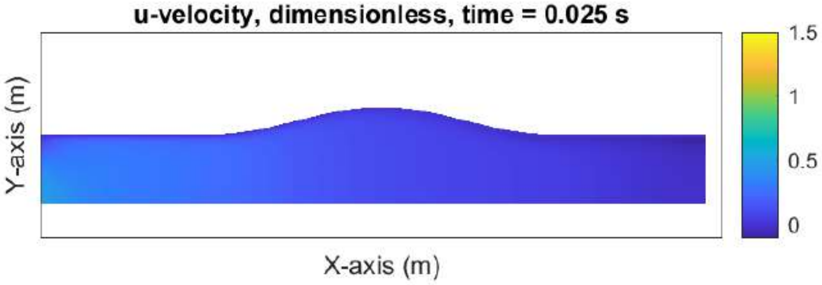

video

Streamlines

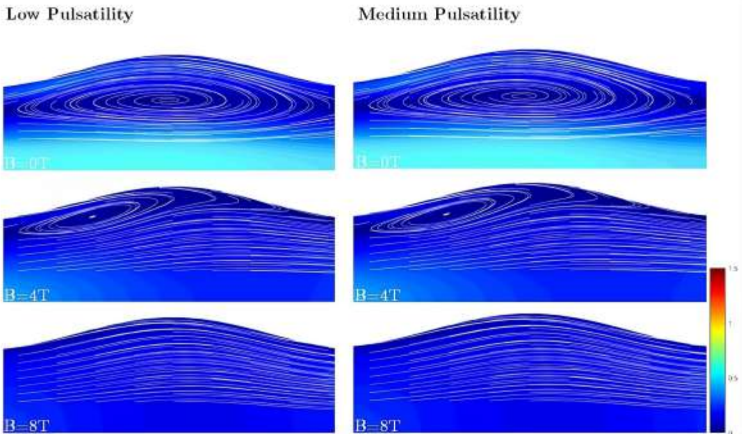

Figure 6: Flow with low and medium pulsatility during systole for $B = 0, 4, 8T$.

Velocity and Pressure Changes

Avg Velocity	Systolic Acceleration		Systolic Deceleration		Diastole	
	Vel	Decrease (%)	Vel	Decrease (%)	Vel	Decrease (%)
B = 0T	0.5720	-	0.4566	-	0.4279	-
B = 4T	0.5659	1.06	0.4511	1.20	0.4211	1.58
B = 8T	0.5638	1.43	0.4479	1.90	0.4178	2.36

Avg Pressure	Systolic Acceleration		Systolic Deceleration		Diastole	
	Pres	Increase (%)	Pres	Increase (%)	Pres	Increase (%)
B = 0T	1.0951	-	-1.8691	-	1.0025	-
B = 4T	1.3584	24.04	-1.4558	22.11	2.0294	102.43
B = 8T	2.0530	87.47	-0.2503	86.60	5.3087	429.54

Table 1: Velocity and Pressure changes for the fourth cardiac cycle for medium pulsatility.

The WSS is a metric to quantify the frictional forces acting on the abdominal aortic aneurysm wall.

$$\tau_{wall} = \frac{\mu R}{u_0}\left(\frac{\partial u}{\partial y} + \frac{\partial v}{\partial x}\right) \tag{12}$$

Avg WSS	Systolic Phase		Diastolic Phase	
	Low	Medium	Low	Medium
B = 4T	13.19	22.22	31.73	34.39
B = 8T	35.16	31.94	67.06	74.52

Table 2: Average WSS values.

Velocity Profile

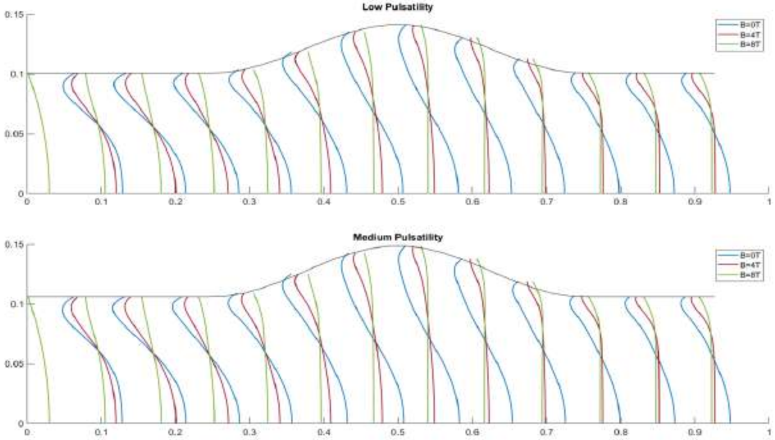

Figure 7: Velocity profile for$B = 0, 4, 8T$.

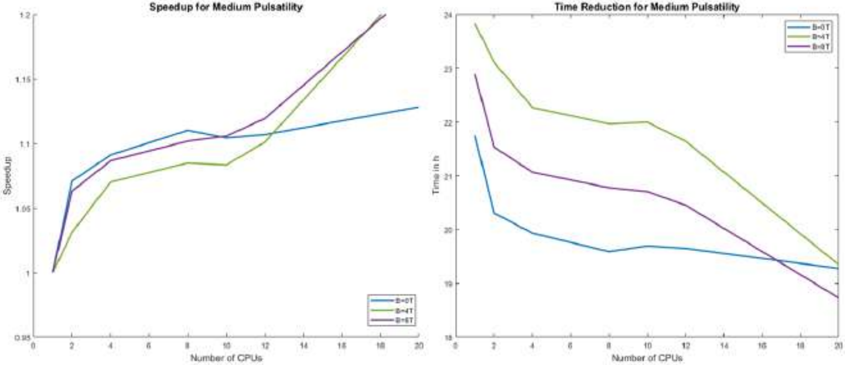

Figure 8: Speedup test and time reduction for medium pulsatility results for 1 — 20 CPUs.

Conclusions

Conclusions

In this study we:

- focused on the $2D$ Navier-Stokes equations and utilizing the Generalized Curvilinear Coordinates and the Finite Volume Method.
- analysed the changes that occur under the presence of the magnetic field on a biomedical application.
- examined the velocity and pressure fields and noticed a substantial influence by the pulsating wall and the magnetic field.

Future Steps

Our next goals are:

- extend our research in a *3D* model.
- add magnetic field in all dimensions so it could better describe an MRI scan.

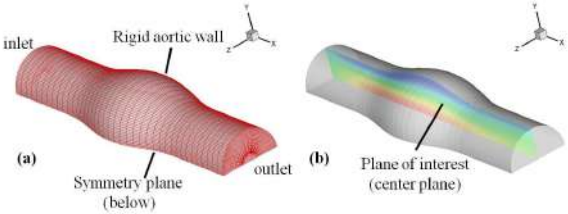

Bibliography i

1. Kyriakoudi, K. C. & Xenos, M. A. **Magnetohydrodynamic effects on a pathological vessel: An Euler–Lagrange approach.** *Physics of Fluids* **35** (2023).
2. Raptis, A., Xenos, M., Tzirtzilakis, E. & Matsagkas, M. **Finite element analysis of magnetohydrodynamic effects on blood flow in an aneurysmal geometry.** *Physics of Fluids* **26,** 101901 (2014).
3. Sakalihasan, N., Limet, R. & Defawe, O. D. **Abdominal aortic aneurysm.** *The Lancet* **365,** 1577–1589 (2005).
4. Shyy, W. & Vu, T. C. **On the adoption of velocity variable and grid system for fluid flow computation in curvilinear coordinates.** *Journal of Computational Physics* **92,** 82–105 (1991).
5. Xenos, M. **An Euler–Lagrange approach for studying blood flow in an aneurysmal geometry.** *Proceedings of the Royal Society A: Mathematical, Physical and Engineering Sciences* **473,** 20160774 (2017).

Thank you!

Questions?

k.kyriakoudi@uoi.gr